Nano World Journal

https://doi.org/10.17756/nwj.2023-s2-006

Research Article

Open Access

Influence of Calcined Clay on Workability of Mortars with Low-carbon Cement

Lucia Ferrari[1], Villiam Bortolotti[1], Nikola Mikanovic[2], Mohsen Ben-Haha[2] and Elisa Franzoni[1]

[1]University of Bologna, Department of Civil, Chemical, Environmental and Materials Engineering, via Terracini 28, Bologna, Italy
[2]Global R&D, HeidelbergCement AG, Oberklamweg 2-4, Leimen, Germany

***Correspondence to:**
Lucia Ferrari
University of Bologna,
Department of Civil, Chemical, Environmental and Materials Engineering,
via Terracini 28, Bologna, Italy.
E-mail: lucia.ferrari9@unibo.it

Received: July 25, 2023
Accepted: September 18, 2023
Published: September 21, 2023

Citation: Ferrari L, Bortolotti V, Mikanovic N, Ben-Haha M, Franzoni E. 2023. Influence of Calcined Clay on Workability of Mortars with Low-carbon Cement. *NanoWorld J* 9(S2): S30-S34.

Published by United Scientific Group

Abstract

The second-largest industrial global emitter of CO_2 (Carbon dioxide) is the cement sector. The technology roadmap of low carbon transition for cement industries includes the introduction of calcined clay (CC) as supplementary cementitious material. A new type of alternative binder, called Limestone Calcined Clay Cement (LC^3), was recently proposed. This cement can reduce CO_2 emissions of cement production by up to 40% and it is prepared using limestone (LS) and clay which are globally available. Many scientific studies aimed to investigate the hydration of LC^3 to understand the contribution of CC to the development of the compressive strength. However, recent studies showed that other cement properties, like workability and water demand, are highly impacted by calcined clay. Despite some papers state that an increase in superplasticizer (SP) dosage compensate this effect, such concrete is usually sticky, and hard to handle and deal with. In this sense, a proper understanding of the mechanisms regulating rheology of LC^3 is needed. The objective of this study is to analyze workability of CC-based cement pastes and mortar, specifically investigating the role of free water in particle suspensions. Preliminary results show that CC highly influences workability of mortars and pastes. The flow table test results highlight a need to increase SP dosage to achieve target workability with CC cements. Differential scanning calorimetry (DSC) and ^{1}H time domain-nuclear magnetic resonance (TD-NMR) results clarify that the capillary unbound water is rapidly consumed by CC, being thus unavailable to fluidify cement pastes. This multi-method approach provides a further step in understanding CC impact on workability of mortars with low-carbon cement and opens new ways to understand paste, mortar, and concrete workability.

Keywords

Calcined clay, Limestone calcined clay cement, Mortar rheology, Differential scanning calorimetry, ^{1}H time domain-nuclear magnetic resonance

Introduction

Concrete is the most widely used building material for infrastructures and buildings. Cement, concrete's key ingredient, has a dramatic carbon footprint as clinker production is responsible for about 7% of the world's CO_2 emissions. For this reason, European Standard EN 197-5:2021 was published in May 2021 to allow formulation of cement of class CEM II/C-M containing from 50% to 64% of clinker, while previous version CEM II/B allowed at minimum 65% of clinker. This paves the path to the use of LC^3, a binder whose features have been studied over the last few years in terms of chemistry and material hydration, showing that this material has promising properties concerning cement reactivity and sustainability [1].

However, workability studies showed that concrete viscosity is higher with binder containing CC and slump retention performance of concrete with LC^3 is poorer than concrete prepared with ordinary Portland cement [2]. Moreover, the increase of CC content decreases initial slump values of concrete [3]. Few studies concern the negative impact of CC on SP efficiency to improve paste workability [4-6]. Furthermore, it was shown that CC is the main factor contributing to the increase of viscosity, yield stress, initial thixotropy [7]. A recent study from Hou et al. [8] combined rheological study with ^{1}H TD-NMR analysis, showing that CC increases static yield stress of pastes and more free water is available in LS sample in comparison to sample containing LS and CC. The interaction between water and CC deserves specific attention to understand the impact of this material on the rheology of paste, mortar, and concrete.

In the present article, the analysis of mortar workability was performed by the flow table test on standard composition with different CC proportions. Different types of samples were prepared: mortar samples, with a water-to-binder ratio w/b = 0.5, and cement paste samples, with a w/b = 0.4. A commercial CEM I and CEM II were used to establish the reference flow parameters of mortars. Different mortars with variable proportions of CEM I, LS and CC were prepared using a SP to obtain target workability measured by flow table tests. In a second moment, capillary unbound water in paste was detected by means of DSC and 1H TD-NMR, a low field NMR approach. The combination of these techniques enabled a further understanding of the impact of CC on the rheology of paste, mortar, and consequently concrete.

Materials and Method

Materials

The materials to blend low carbon cements and aggregates were supplied by Heidelberg Materials. The binders and powders used in this study were: Milke® CEM I 52.5 R (CEM I) from HeidelebergMaterials Geseke plant, CEM II/A-LL is based on Geseke clinker and WK mehl LS filler contained at 12% (CEM II), CC from France, and LS. The polycarboxylate ether-based SPs used in this study was gently provided by CHRYSO SAINT-GOBAIN R&D laboratory in Sermaises (France) and contains 22% of solid. The chemical composition of materials obtained by XRF analysis is reported in table 1. The materials used (CC, binders, and powders) were nanoscale.

Particle size distribution was measured by laser diffraction. CEM I and CEM II were investigated by Malvern Mastersizer 3000, in isopropanol, while LS and CC were tested in water by a Malvern Hydro 2000MU (A). The finesses of binders and powders are reported in table 2. The four powders are characterized by similar grain size distribution, except for LS that is slightly coarser.

The sand exhibits a maximum particle diameter of 4 mm. Tests to characterize sand were conducted according to EN 1097-6 standard specification. The measured oven-dried particle density of sand is (2.66 ± 0.02) g/cm^3, while measured water absorption percentage is (0.44 ± 0.02).

Table 1: Chemical composition of CEM I, CEM II, and CC.

Chemical formula	Unit	CEM I	CEM I	CC
LOI 1050 °C	%	2.49	5.74	2.36
SiO_2	%	19.24	18.12	60.24
Al_2O_3	%	5.12	4.80	25.79
TiO_2	%	0.29	0.28	1.26
MnO	%	0.04	0.03	0.00
Fe_2O_3	%	3.22	3.02	8.87
CaO	%	62.69	61.44	0.98
MgO	%	1.89	1.67	0.24
K_2O	%	1.02	1.04	0.17
Na_2O	%	0.07	0.06	0.00
SO_3	%	3.32	3.24	0.05
P_2O_5	%	0.14	0.16	0.02
Sum-RFA (1050 °C)	%	99.51	99.60	99.99

Formulation

Binder formulation

The two commercial cements, CEM I and CEM II, were used as reference binders. Other three binders were formulated according to the following proportions:

- LC^3-50 2:1 with 50% of clinker, CC:LS = 2:1
- LC^3-50 1:1 with 50% of clinker, CC:LS = 1:1
- LC^3-70 2:1 with 70% of clinker, CC:LS = 2:1

The clinker was supplied to the blends of LC^3 by inserting CEM I in the mixes and considering the amount of clinker in CEM I equal to 95%, the rest being calcium sulfate.

Mortar preparation

The mortar preparation and mixing were conducted in a Hobart mixer, according to standard EN 196-1:2016. The composition was 450 ± 2 g of binder, 1350 ± 5 g of analyzed sand, 225 ± 1 g of water. The SP dosage was adjusted to provide target flowability.

Paste preparation

Paste preparation was implemented starting from EN 196-11:2016 and adapted to Quiet stirred system. The composition was 50.0 ± 0.2 g of binder and 20.0 ± 0.2 g of water. The water and the cement were placed into the bowl and mixed for 1 min at low speed (1800 rpm). Afterwards, the mixing speed was increased to 3000 rpm for 30 s then stopped for 90 s. During this time, the mortar adhering to the wall and bottom part of the bowl was removed by means of a rubber or plastics scraper. Finally, the mixing continued at high speed (3000 rpm) for 60 s.

Table 2: Granulometry of binders and powders (D10, D50 and D90 are the diameters corresponding to 10 vol%, 50 vol% and 90 vol% of the material).

Material	D10 (µm)	D50 (µm)	D90 (µm)
CEM I	2.11	11.1	32.4
CEM II	1.84	12.9	46.9
LS	4.82	30.0	135
CC	2.39	17.1	55.1

Methodology

Flow test on mortar

Mortar flow immediately after mixing was measured by flow table test according to ASTM C-1437 standard specification. A mortar spread between 200 and 220 mm was targeted by using an appropriate SP dosage to obtain a mortar which is neither too sticky to allow good flow, nor too liquid to avoid segregation.

Thermal analysis of paste by DSC

DSC allowed the detection of the free water in pastes 10 min after mixing [9]. The idea is to freeze the free water in a cement paste and to measure the enthalpy of melting water during the subsequent heating. The measured enthalpy is considered as a quantification of the amount free water remaining in cement paste. The measurements were conducted using a Q10 DSC TA Instruments, with aluminum hermetic pans. Roughly 20 mg of the prepared paste was transferred into the pan, and it was hermetically closed. The reference pan was kept empty as usual for measurements with DSC. The temperature program was adjusted starting from the approach proposed by Ridi et al. [10] and it was as following: equilibrate at -30 °C, isothermal for 1 min, from -30 °C to -12 °C an increasing ramp at 20 °C/min, from -12 °C to +35 °C another increasing ramp at 4 °C/min.

The percentage of consumed water in pastes prepared with the same w/b = 0.4, after 10 min of hydration, is calculated as:

$$Consumed\ water\ \% = 100 - \Delta H_{exp} / (\phi_w \Delta H_{theor})$$

Where, ΔH_{exp} is the area of the water melting peak, ϕ_w is the weight fraction of water in the paste and ΔH_{theor} is the theoretical value of the enthalpy of melting water, i.e. 334 J/g.

Water detection in paste by ^{1}H TD-NMR

The objective of NMR measurements was to detect the amount of capillary, interhydrate and interlayer water in pastes. NMR equipment allows the detection of the transverse (T_2) relaxation curves and the computed values of T_2 provide information about water confinement in cement matrix and porous media in general.

The instrumental setup is composed of a permanent magnet (ARTOSCAN-ESAOTE, Genova, Italy) with a magnetic field $B_0 \approx 0.2$ T (corresponding to ^{1}H Larmor frequency ≈ 8 MHz), a 10 mm probe, and an NMR console (Stelar s.r.l., Mede, Italy).

Relaxation time T_2 was detected using the Carr-Purcell-Meiboom-Gill sequence with 512 - 1024 number of echoes, depending on the saturation level of the samples, with an echo time of 60 µs and 500 scans. Data acquisitions were conducted at 1 h of hydration and two repeated measurements were performed on each sample.

The T_2 quasi-continuous distribution was computed by the software UpenWin [11], developed by the group at University of Bologna, to verify the presence of specific peaks, while for non-linear fitting a script in Psi-Plot was implemented [12]. For tri-exponential fitting, the T_2, the corresponding assignment and pore size are reported in table 3, according to previous studies carried out on white cement [1].

Results and Discussion

Table 3: T_2 values, corresponding assignment and pore size used for tri-exponential fitting.

T_2 (ms)	Pore size (nm)	Assignment
8 - 10	~1000	Capillary water
1 - 2	10 - 20	Interhydrate water
0.1 - 0.2	3 - 5	Interlayer water

Mortar flow property

SP dosage to obtain target average diameter of mortar with different binders after 25 drops at the flow table is reported in table 4.

It has to be noted that SP dosage increases with the amount of CC in the binder, and the resulting correlation factor is $R^2 = 0.9983$.

Table 4: SP dosage to obtain target average diameter of mortar (200 - 220 mm) with different binders after 25 drops at the flow table.

Binder	SP dosage (g SP/g binder)	Average diameter (mm)
CEM I	0.6%	213
CEM II	0.6%	210
LC^3-50 2:1	1.3%	207
LC^3-50 1:1	1.1%	214
LC^3-70 2:1	1.0%	218

Detection of consumed water in fresh paste by DSC

The thermal analysis by DSC revealed that the amount of consumed water after 10 min of hydration is different for each binder, as shown in figure 1.

In average, the amount of consumed water is around 20% for all the samples. It has to be noted that this DSC method detects exclusively capillary water and does not detect the water contained in smaller pores. Most probably, a part of the water forms the early hydrates (like ettringite that precipitates immediately after mixing), and another part starts to form the

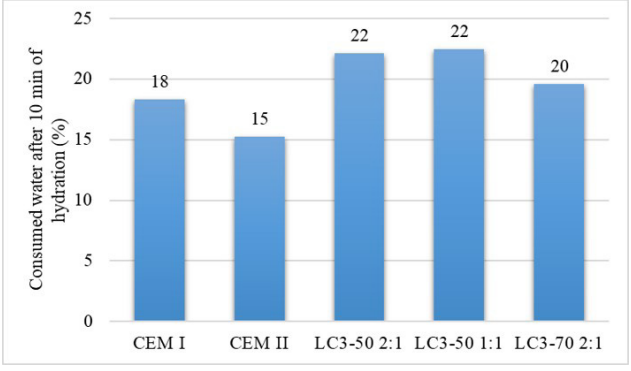

Figure 1: Percentage of consumed water in pastes prepared with different binders at the same w/b = 0.4 after 10 min of hydration.

first small pores. These two portions of water are both invisible to DSC.

Concerning the different binders, CEM II consumes less water than CEM I as it contains less clinker, and the hydration kinetics is slower. However, for the LC^3 binders, the consumption of water is comparable to or higher than CEM I despite the lower clinker content. This result suggests that part of the water used for the paste preparation disappears as soon as it gets in contact with the CC. This water is probably sucked or trapped into clay microstructure, increasing the solid volume fraction of paste with drastic consequences on paste rheology.

Water detection by ^{1}H TD-NMR

The T_2 quasi-continuous distribution computed by the software UpenWin revealed the presence of two main peaks around 10 ms and 2 ms (Figure 2). A third peak around 0.2 ms is slightly visible but it was neglectable after the triexponential fitting. According to the literature [13], these peaks correspond to capillary water (pores of nearly 1 µm), interhydrate water (pores of about 10 - 20 nm) and gel pores (3 - 5 nm).

The percentage of capillary water and interhydrate water in pastes after 1 h of hydration for different binders is shown in figure 3. These results highlight that, on one hand, CEM I and CEM II show a relatively high percentage of capillary water and low percentage of interhydrate water; on the other hand, LC^3 immediately trap initial capillary water generating high percentage of interhydrate water, i.e., pores of nearly 10 - 20 nm.

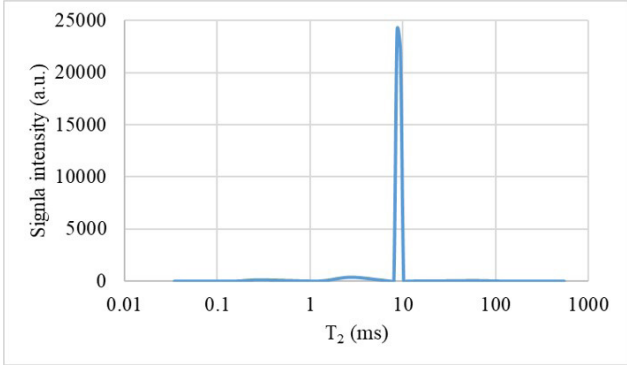

Figure 2: T_2 quasi-continuous distribution computed by the software UpenWin for paste of CEM I after 1 h of hydration.

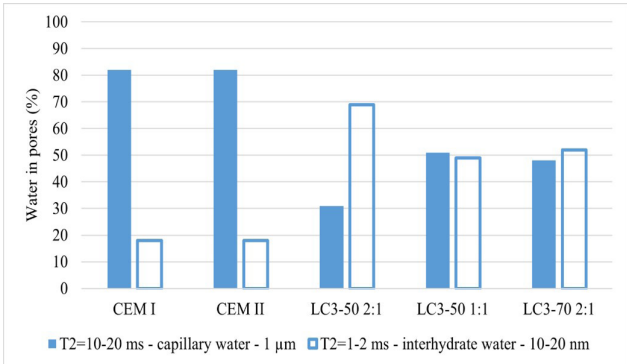

Figure 3: Percentage of capillary water and interhydrate water detected by ^{1}H TD-NMR after 1 h of hydration.

These results agree with what was highlighted by the thermal analysis and mortar tests. Apparently, CC cement consumes free water more rapidly than commercial CEM I and CEM II cements, with direct consequences on cement demand and workability retention of paste, mortar, and concrete. Moreover, NMR confirmed the high consumption of capillary water by CC and consequent formation of pores measuring approximately 10 - 20 nm in size. Further studies on the interaction between pure CC and water will help to understand this phenomenon and support new possibility to prevent workability loss of CC-based cement.

Conclusion

The present article deals with the influence of binder composition on mortar rheology, also quantifying the amount of consumed water in the cement paste in the very beginning of hydration. More specifically, blends containing CC and LS were formulated with different proportions to detect the impact of these powders on the workability of mortar. A specific study was conducted on paste by DSC and ^{1}H TD-NMR to understand the role of unbound water and consumed water on rheological properties of mortar. The results obtained with the flow table test allowed to directly relate the SP dosage to reach target workability to the amount of CC contained in the binder. The correlation coefficient close to 1 confirmed that CC has a drastic impact on rheological properties of new low carbon cements. The thermal analysis by DSC after 10 min of hydration showed that cements containing CC consume a higher amount of free water than CEM I and CEM II. This effect suggests the idea that a specific interaction between CC and water is occurring since the first contact of the two materials. One hypothesis may be that water is trapped in the structure of CC or sucked in it. However, further investigations are required to better understand and quantify the water bound by CC. The ^{1}H TD-NMR confirmed the results from DSC, additionally showing that the unbound water consumed in the first hour of hydration is hidden in interhydrate pores, corresponding to pore size of 10 - 20 nm. These results provide a starting point for further investigations into the role of water in new low carbon cements. Indeed, the parameters affecting this significant water consumption and how to prevent or limit this negative effect on concrete workability are relevant and unneglectable aspects for CC application.

Acknowledgments

Paolo Carta from University of Bologna is warmly thanked for his support during laboratory tests. Giovanni Ridolfi from CentroCeramico is thanked for providing the analysis of particle size distribution of calcined clay and limestone.

Conflict of Interest

The authors wish to confirm that there are no known conflicts of interest associated with this publication.

Funding

The authors would like to acknowledge Heidelberg Materials for financial and technical support.

References

1. Scrivener K, Avet F, Maraghechi H, Zunino F, Ston J, et al. 2018. Impacting factors and properties of limestone calcined clay cements (LC^3). *Green Mater* 7(1): 3-14. https://doi.org/10.1680/jgrma.18.00029
2. Nair N, Haneefa KM, Santhanam M, Gettu R. 2020. A study on fresh properties of limestone calcined clay blended cementitious systems. *Constr Build Mater* 254: 119326. https://doi.org/10.1016/j.conbuildmat.2020.119326
3. Nguyen QD, Khan MSH, Castel A. 2018. Engineering properties of limestone calcined clay concrete. *J Adv Concr Technol* 16(8): 343-357. https://doi.org/10.3151/jact.16.343
4. Li R, Lei L, Sui T, Plank J. 2021. Approaches to achieve fluidity retention in low-carbon calcined clay blended cements. *J Clean Prod* 311: 127770. https://doi.org/10.1016/j.jclepro.2021.127770
5. Li R, Lei L, Sui T, Plank J. 2021. Effectiveness of PCE superplasticizers in calcined clay blended cements. *Cem Concr Res* 141: 106334. https://doi.org/10.1016/j.cemconres.2020.106334
6. Schmid M, Plank J. 2020. Dispersing performance of different kinds of polycarboxylate (PCE) superplasticizers in cement blended with a calcined clay. *Constr Build Mater* 258: 119576. https://doi.org/10.1016/j.conbuildmat.2020.119576
7. Muzenda TR, Hou P, Kawashima S, Sui T, Cheng X. 2020. The role of limestone and calcined clay on the rheological properties of LC^3. *Cem Concr Compos* 107: 103516. https://doi.org/10.1016/j.cemconcomp.2020.103516
8. Hou P, Muzenda TR, Li Q, Chen H, Kawashima S, et al. 2021. Mechanisms dominating thixotropy in limestone calcined clay cement (LC^3). *Cem Concr Res* 140: 106316. https://doi.org/10.1016/j.cemconres.2020.106316
9. Ridi F, Fratini E, Luciani P, Winnefeld F, Baglioni P. 2011. Hydration kinetics of tricalcium silicate by calorimetric methods. *J Colloid Interface Sci* 364(1): 118-124. https://doi.org/10.1016/j.jcis.2011.08.010
10. Ridi F, Fratini E, Luciani P, Winnefeld F, Baglioni P. 2012. Tricalcium silicate hydration reaction in the presence of comb-shaped superplasticizers: boundary nucleation and growth model applied to polymer-modified pastes. *J Phys Chem C* 116(20): 10887-10895. https://doi.org/10.1021/jp209156n
11. Borgia GC, Brown RJS, Fantazzini P. 2000. Uniform-penalty inversion of multiexponential decay data: II. Data spacing, T2 data, systematic data errors, and diagnostics. *J Magn Reson* 147(2): 273-285. https://doi.org/10.1006/jmre.2000.2197
12. James F. 2004. MINUIT Tutorial - Function Minimization. CERN, Geneva.
13. Scrivener K, Snellings R, Lothenbach B. 2018. A Practical Guide to Microstructural Analysis of Cementitious Materials. CRC Press, Boca Raton.